




# Hypoxia induces downregulation of the tumor-suppressive sST2 in colorectal cancer cells via the HIF–nuclear IL-33–GATA3 pathway

Miho Akimoto<sup>a,1</sup> , Takao Susa<sup>a</sup>, Noriyuki Okudaira<sup>a</sup>, Nobuko Koshikawa<sup>b</sup> , Harumi Hisaki<sup>a</sup>, Masayoshi Iizuka<sup>a,c</sup>, Hiroko Okinaga<sup>d</sup>, Keizo Takenaga<sup>b</sup> , Tomoki Okazaki<sup>a</sup>, and Mimi Tamamori-Adachi<sup>a</sup>

Edited by Philippe Krebs, Universitat Bern, Bern, Switzerland; received October 22, 2022; accepted March 30, 2023 by Editorial Board Member Tadatsugu Taniguchi

**As a decoy receptor, soluble ST2 (sST2) interferes with the function of the inflammatory cytokine interleukin (IL)-33. Decreased sST2 expression in colorectal cancer (CRC) cells promotes tumor growth via IL-33-mediated bioprocesses in the tumor microenvironment. In this study, we discovered that hypoxia reduced sST2 expression in CRC cells and explored the associated molecular mechanisms, including the expression of key regulators of ST2 gene transcription in hypoxic CRC cells. In addition, the effect of the recovery of sST2 expression in hypoxic tumor regions on malignant progression was investigated using mouse CRC cells engineered to express sST2 in response to hypoxia. Our results indicated that hypoxia-dependent increases in nuclear IL-33 interfered with the transactivation activity of GATA3 for ST2 gene transcription. Most importantly, hypoxia-responsive sST2 restoration in hypoxic tumor regions corrected the inflammatory microenvironment and suppressed tumor growth and lung metastasis. These results indicate that strategies targeting sST2 in hypoxic tumor regions could be effective for treating malignant CRC.**

colorectal cancer | interleukin-33 | soluble ST2 | metastasis | hypoxia

Colorectal cancer (CRC) is the third most common cancer globally; in the future, its incidence is forecast to further increase. In 2020, approximately 1.9 million new CRC cases were recorded worldwide, accounting for 10% of all cancer cases. CRC is the second leading cause of cancer-related death, causing an estimated 900,000 deaths in 2020 (1). Because the malignant progression of CRC is closely associated with chronic inflammation, a better understanding of the inflammatory tumor microenvironment of CRC is essential for developing more effective therapeutic approaches.

Interleukin (IL)-33 is a member of the IL-1 family and a natural ligand for the membrane-bound IL-33 receptor ST2 (ST2L) (2). IL-33, similar to HMGB1 and IL-1 $\alpha$ , is a dual-function protein that performs distinct intracellular and extracellular functions (3). Full-length IL-33 (fIL-33) functions in transcriptional repression as a nuclear factor. On the contrary, cleaved IL-33 (cIL-33) is released extracellularly as an inflammatory cytokine in response to miscellaneous stimuli, binding to ST2L on the target cell membrane to induce various signaling pathways. ST2 has multiple splicing variants; among them, soluble ST2 (sST2) functions as a decoy receptor, inhibiting IL-33 binding to ST2L (4). Because the IL-33–ST2L axis mainly induces Th2 responses, many studies have examined its association with various chronic inflammatory diseases (5), including atopic dermatitis (6, 7), asthma (8–10), rheumatoid arthritis (11, 12), and chronic inflammatory bowel diseases (13, 14). Of particular interest, the involvement of the IL-33–ST2L axis in malignant progression has been reported in breast cancer (15, 16), liver cancer (17, 18), gastric cancer (19), lung cancer (20, 21), and intestinal cancers including CRC (22–29). Serum sST2 levels in ER-positive breast cancer patients are associated with poor prognosis (30). Furthermore, IL-33 is involved in Treg cell-mediated tumor immunoevasion (31). We previously reported that sST2 levels are inversely associated with the metastatic potential of CRC cells and that reduced sST2 expression in CRC cells promotes IL-33/ST2L-mediated bioprocesses, such as Th2 differentiation, macrophage infiltration, and angiogenesis, to enhance tumor growth and metastasis (32). Thus, the quantitative balance between IL-33 and sST2 in CRC tumors has a great influence on malignant progression.

Hypoxia is closely associated with the malignant progression of various cancers, including CRC (33–35). In the hypoxic tumor regions that emerge during tumor growth, the expression of several cytokines, chemokines, and other hypoxia-responsive genes is induced in tumor cells and tumor stromal cells, producing a cancer-promoting inflammatory

## Significance

In the tumor microenvironment of colorectal cancer (CRC), sST2 acts in a tumor-suppressive manner by inhibiting the proinflammatory function of interleukin (IL)-33. This study demonstrates that hypoxia, which is closely associated with tumor malignancy, decreases sST2 expression in CRC cells. Hypoxia-induced sST2 depletion results from hypoxia-inducible factor-dependent nuclear accumulation of IL-33, which binds to GATA3 and blocks its access to the sST2 promoter. Most importantly, restoration of sST2 expression limited to hypoxic regions in mouse CRC tumors improves the inflammatory tumor environment, effectively suppressing tumor growth and metastasis. sST2 depletion is also observed in hypoxic regions of human CRC lesions. Our findings suggest that sST2 enhancement specifically targeting hypoxic tumor regions may be useful in the treatment of malignant CRC.

The authors declare no competing interest.

This article is a PNAS Direct Submission. P.K. is a guest editor invited by the Editorial Board.

Copyright © 2023 the Author(s). Published by PNAS. This article is distributed under [Creative Commons Attribution-NonCommercial-NoDerivatives License 4.0 \(CC BY-NC-ND\)](https://creativecommons.org/licenses/by-nc-nd/4.0/).

<sup>1</sup>To whom correspondence may be addressed. Email: [mihoaki@med.teikyo-u.ac.jp](mailto:mihoaki@med.teikyo-u.ac.jp).

This article contains supporting information online at <https://www.pnas.org/lookup/suppl/doi:10.1073/pnas.2218033120/-/DCSupplemental>.

Published April 24, 2023.

microenvironment. This is mainly mediated by hypoxia-inducible factor (HIF)-1 and HIF-2, which are heterodimers consisting of an oxygen-sensitive HIF-1 $\alpha$  or HIF-2 $\alpha$  subunit and a constitutively expressed HIF- $\beta$  subunit (36, 37). However, to our knowledge, there are no reports detailing sST2 expression in tumor hypoxic regions and its effect on malignancy.

Human and rodent ST2 gene expression is controlled by the distal promoter upstream of exon 1a and the proximal promoter between exons 1a and 1b (38, 39). Promoter preference depends on cell type and situation but is independent of the type of ST2 splicing variant. For example, most sST2 and ST2L expression in mouse mast cells is regulated by the distal promoter, whereas the expression of both variants in mouse fibroblasts is regulated by the proximal promoter (40, 41). The human and mouse ST2 distal promoters have several common GATA consensus sites, especially two sites immediately upstream of the transcription start site, which are believed to be particularly important for transcriptional activity (40, 42). In fact, the ST2 distal promoter is regulated by GATA family proteins (GATA1, GATA2, and GATA3) in LAD2 human mast cell leukemia cells, KU812 human basophilic leukemia cells, and mouse thoracic adenoma cells (42, 43). However, which GATA molecules bind to which GATA sites and repress or activate ST2L or sST2 gene expression remains unclear. In addition, STAT3 binds to the serum response element in the ST2 proximal promoter and induces gene expression via activation of the ERK pathway in response to cell proliferation stimulation or mutant Ras (44).

fIL-33 has a nuclear localization signal and a homeodomain that binds to the H2A–H2B pockets on the surface of heterochromatin and nucleosomes (45). The structure of fIL-33 suggests that it enhances interactions between nucleosomes, promotes chromatin aggregation, and functions as a repressor (45, 46). Shao et al. reported that nuclear IL-33 binds directly to multiple homeoboxes within the ST2 promoter and suppresses sST2 expression by recruiting the methyltransferase SUV39H1, which mediates histone H3K9 trimethylation (H3K9me3) (47).

In this study, we investigated the effects of hypoxia on sST2 expression in CRC cells and those of hypoxia-induced changes in sST2 expression on cell malignancy. We revealed decreased sST2 expression in hypoxic CRC cells via the HIF–IL-33–GATA3 axis and sST2 downregulation in the hypoxic regions of mouse and human CRC tumors. Importantly, we provided evidence that restoration of sST2 expression in those regions corrected the inflammatory tumor microenvironment and suppressed tumor growth and metastasis.

## Results

**sST2 Expression in CRC Cells Is Suppressed by HIF Activation.** ST2L and sST2 levels in NM11 mouse CRC cells and SW480 human CRC cells under hypoxic conditions were investigated by qRT-PCR. The basal mRNA levels of sST2 in both cells were much higher than those of ST2L and significantly decreased in a time-dependent manner for up to 24 h under hypoxic conditions (1% O<sub>2</sub>; Fig. 1*A* and *SI Appendix, Fig. S1A*). sST2 mRNA levels remained low under long-term hypoxia (Fig. 1*B* and *SI Appendix, Fig. S1B*). Consistent with the decrease in mRNA levels, sST2 protein levels in culture supernatants were lower under hypoxic conditions than those under normoxic conditions (Fig. 1*C* and *SI Appendix, Fig. S1C*). These data suggest that sST2 expression is repressed in a hypoxic environment. To clarify whether HIF is involved in the hypoxia-induced sST2 downregulation, we performed siRNA-mediated depletion of HIF-1 $\alpha$  and HIF-2 $\alpha$  in NM11 cells. Decreased sST2 expression in hypoxic NM11

cells was partially restored by HIF-1 $\alpha$  or HIF-2 $\alpha$  depletion and more significantly increased by the depletion of both (Fig. 1*D–F*). In support of these findings, LW6, which promotes HIF-1 $\alpha$  proteolysis without affecting its mRNA levels (48), and TC-S 7009, which suppresses HIF-2 $\alpha$  activity without affecting its protein levels (49), attenuated the decreased sST2 expression in hypoxic NM11 cells (Fig. 1*G* and *H*). In contrast, hypoxia mimetics such as CoCl<sub>2</sub>, desferrioxamine (DFO), and dimethylxaloylglycine (DMOG), which stabilize HIF-1 $\alpha$  and HIF-2 $\alpha$  under normoxic conditions, suppressed sST2 expression (Fig. 1*I* and *J*). Taken together, sST2 expression is suppressed in hypoxic CRC cells partly through HIF- $\alpha$  activation.

**IL-33 Is HIF-Dependently Up-Regulated and Accumulated in the Nucleus.** It has been reported that IL-33 expression is directly or indirectly regulated by HIF-1 $\alpha$  (12, 50). Under hypoxia, unlike the persistent sST2 downregulation, IL-33 mRNA levels in NM11 cells increased for up to 9 h and returned to basal levels by 24 h (Fig. 2*A*). Examination of IL-33 protein levels in the subcellular fractions of hypoxic NM11 cells revealed that fIL-33 (~30 kDa) accumulated in the nucleus, while secretory cIL-33 (18 kDa) was not detected (Fig. 2*B*). fIL-33 increased prior to the decrease in sST2 and appeared to behave like HIF-1 $\alpha$  rather than HIF-2 $\alpha$ . In addition, transient nuclear accumulation of fIL-33 due to hypoxia was confirmed by immunofluorescence staining (*SI Appendix, Fig. S2*). In long-term hypoxic cultures, nuclear IL-33 remained at high levels after a transient increase, consistent with its mRNA levels (*SI Appendix, Fig. S3*). The elevated expression and nuclear accumulation of IL-33 in hypoxic NM11 cells were suppressed by HIF- $\alpha$  depletion or HIF inhibition (Fig. 2*C–F* and *SI Appendix, Fig. S4 A and B*); effects reproduced by treatment with HIF activators under normoxia (Fig. 2*G* and *H* and *SI Appendix, Fig. S4C*). These results suggest that IL-33 is up-regulated in a HIF-dependent manner in hypoxic CRC cells and that it accumulates in the nucleus prior to sST2 downregulation.

**IL-33 Is Involved in Hypoxia-Induced sST2 Downregulation through Transcriptional Suppression of the ST2 Gene.** In hypoxic NM11 cells, the effect of IL-33 siRNA was attenuated by increased expression of endogenous IL-33, but IL-33 depletion could still significantly restore sST2 expression under hypoxia (Fig. 3*A–C*). These data suggest that IL-33 is involved in hypoxia-induced sST2 downregulation. Nuclear IL-33 has been suggested to act as a chromatin-related protein that regulates gene expression by modifying chromatin remodeling (45, 47). Thus, we then examined whether IL-33 affects ST2 gene transcription under hypoxia. The human and mouse ST2 genes (*IL1RL1* and *Il1rl1*, respectively) have distal and proximal promoters that are used depending on the cellular conditions, regardless of isoform type (*SI Appendix, Fig. S5A*) (40, 41). The use of the human ST2 distal and proximal promoters under hypoxic conditions was examined by a dual-luciferase reporter assay using HEK293 cells (*SI Appendix, Fig. S5B*). Proximal promoter activity was significantly higher than distal promoter activity regardless of the oxygen concentration, but neither promoter activity differed between normoxic and hypoxic conditions (*SI Appendix, Fig. S5C*). However, it should be noted that HEK293 cells are deficient in most IL-33–ST2L axis-related factors, including IL-33, ST2L, sST2, and IL1RAP (*SI Appendix, Fig. S5D*). Thus, we established HEK293 cells exogenously expressing fIL-33 or cIL-33 as negative control. In these cells, cIL-33 localized to the cytoplasm, while fIL-33 accumulated in the nucleus regardless of oxygen status (Fig. 3*D* and *E* and *SI Appendix, Fig. S5E*). Reporter assays using these cells showed that the ST2 proximal promoter activities were

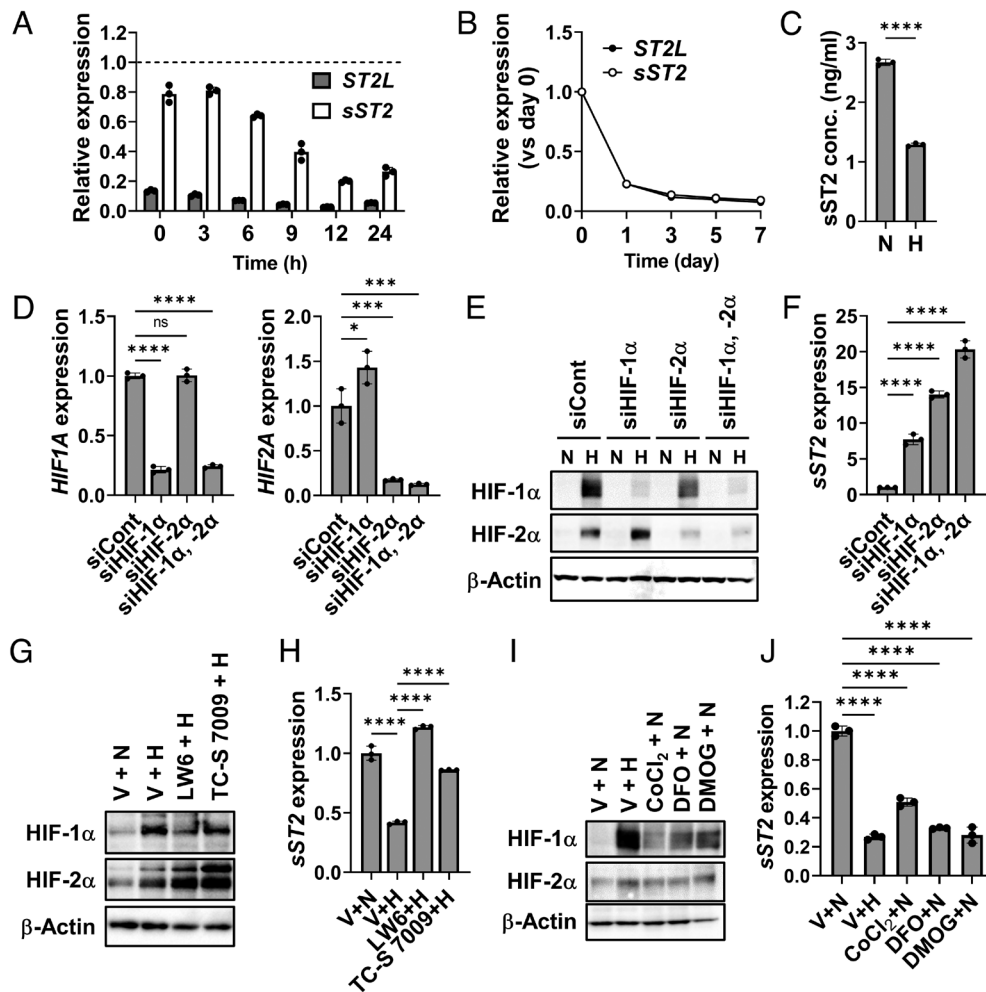


**Fig. 1.** HIFs are involved in regulating sST2 expression in hypoxic CRC cells. (A and B) qRT-PCR showing sST2 and ST2L expression levels in NM11 cells during short-term (A) or long-term (B) hypoxia. All data are presented as relative values. In A, the ST2 isotype-nonspecific qRT-PCR value at 0 h is set to 1 (dotted line); in B, the value at day 0 is set to 1. (C) Enzyme-Linked Immunosorbent Assay (ELISA) showing sST2 concentrations in the culture supernatants of NM11 cells cultured for 3 d under normoxia (N, 21% O<sub>2</sub>) or hypoxia (H, 1% O<sub>2</sub>). (D and E) qRT-PCR (D) and western blotting (E) showing siRNA-mediated HIF- $\alpha$  depletion in NM11 cells. (F) qRT-PCR showing sST2 expression in HIF- $\alpha$ -depleted NM11 cells under hypoxia (1% O<sub>2</sub> 12 h). (G) Western blot images showing HIF- $\alpha$  protein levels in NM11 cells treated with HIF inhibitors. NM11 cells were incubated in the presence of DMSO (vehicle, V) or an HIF-1 $\alpha$  inhibitor (20  $\mu$ M LW6) or an HIF-2 $\alpha$  inhibitor (50  $\mu$ M TC-S 7009) for 12 h followed by another 12 h under normoxia (N) or hypoxia (H). (H) qRT-PCR analysis showing sST2 expression levels under the same conditions as G. (I) Western blot images showing stabilization of HIF-1 $\alpha$  protein levels by hypoxia-mimetic treatment. NM11 cells were cultured under normoxic conditions (21% O<sub>2</sub>, 12 h) in the presence of DMSO (vehicle, V) or an HIF-1 $\alpha$  activator (200  $\mu$ M CoCl<sub>2</sub> or 100  $\mu$ M DFO or 100  $\mu$ M DMOG). (J) qRT-PCR showing sST2 expression levels under the same conditions as I. Data for A–D, F, H, and J are presented as the mean  $\pm$  SD  $n = 3$  of biologically independent samples.  $P$  values were analyzed by unpaired two-tailed  $t$  test for C and by one-way ANOVA with Bonferroni correction for multiple comparisons for D, F, H, and J. \* $P < 0.05$ ; \*\*\* $P < 0.001$ ; \*\*\*\* $P < 0.0001$ ; ns, not significant. The uncropped western blot images are shown in *SI Appendix*.

reduced under hypoxic conditions only in fIL-33-expressing cells (Fig. 3F). Furthermore, treating HEK293 cells with recombinant cIL-33 (rcIL-33) did not reduce ST2 promoter activity under hypoxia (Fig. 3G). Thus, our results suggest that fIL-33, but not cytoplasmic and extracellular cIL-33, is important for the decreased ST2 gene transcription under hypoxia. Notably, despite the accumulation of fIL-33 in the nucleus of HEK293 cells, ST2 proximal promoter activity did not decrease under normoxia, suggesting that other factors are involved in the suppression of sST2 expression caused by hypoxia.

**The Hypoxia-Induced Suppression of ST2 Gene Transcription Is Not Accompanied by H3K9 Trimethylation.** Shao et al. demonstrated that nuclear IL-33 suppresses sST2 expression by recruiting SUV39H1 (47). Therefore, we analyzed the H3K9me3 status at the ST2 distal and proximal promoters of SW480 cells under hypoxic conditions by chromatin immunoprecipitation (ChIP). The results showed higher H3K9me3 levels at the distal promoter than that at the proximal promoter. Its levels increased in a time-dependent

manner under hypoxia (*SI Appendix*, Fig. S6A) and were attenuated by siRNA-mediated IL-33 depletion (*SI Appendix*, Fig. S6B). We also examined the effect of chaetocin, an SUV39H1 inhibitor, on sST2 expression in SW480 cells under hypoxia, and found a recovery of hypoxia-induced sST2 downregulation (*SI Appendix*, Fig. S6C). However, these responses were not specific to hypoxia; in fact, chaetocin treatment also increased sST2 under normoxia. Thus, our results suggest that IL-33 likely regulates the hypoxia-specific sST2 downregulation via factors other than SUV39H1.

**Nuclear IL-33 Binds to GATA3 and Suppresses GATA3-Mediated sST2 Expression under Hypoxia.** Recently, it was reported that nuclear IL-33 binds to transcription factors such as NF- $\kappa$ B and acts as a transcriptional modulator (51). Interestingly, according to STRING (<https://string-db.org/>), an analytical tool for predicting protein–protein interactions, the accuracy of the interaction between IL-33 and the Th2-specific transcription factor GATA3 is extremely high across mammals (*SI Appendix*, Fig. S7). However, no reports have described either direct or indirect protein–protein

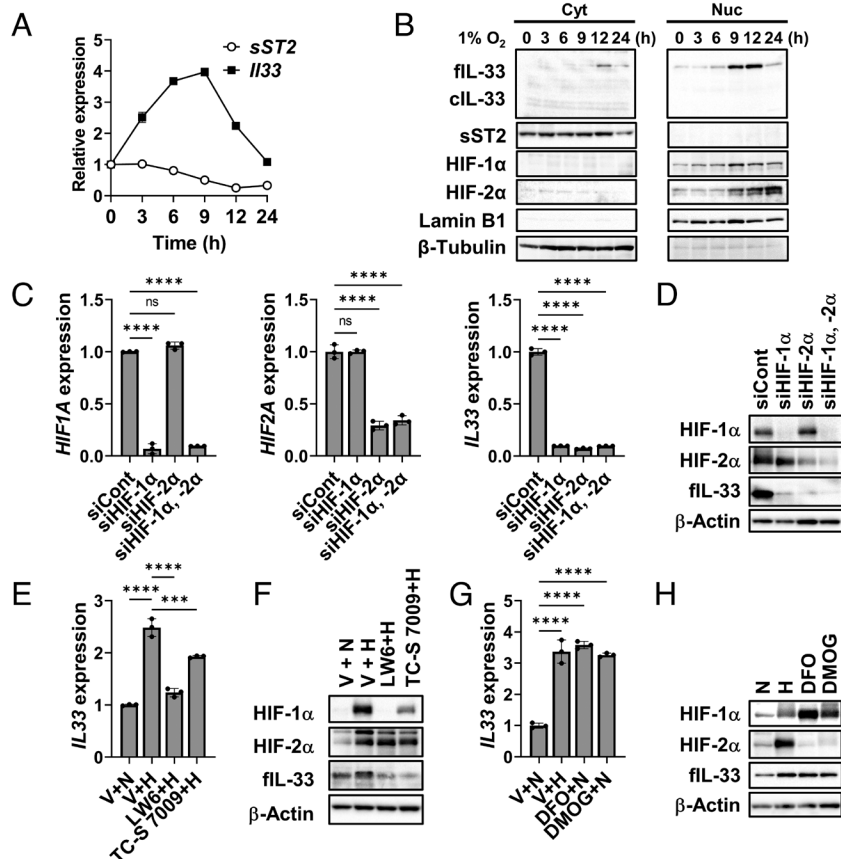


**Fig. 2.** IL-33 is HIF- $\alpha$  dependently up-regulated and accumulates in the nucleus of hypoxic CRC cells. (A) qRT-PCR analysis showing the correlation between IL-33 and sST2 expression levels in NM11 cells under hypoxia. Data are displayed relative to the value at 0 h. (B) Western blotting showing time-dependent changes in the levels of various proteins under hypoxia. Cyt, cytoplasmic fraction; Nuc, nuclear fraction. Beta-tubulin and lamin B1 were used as markers for cytoplasmic and nuclear fractions, respectively. (C and D) qRT-PCR (C) and western blotting (D) showing IL-33 levels in HIF- $\alpha$ -depleted NM11 cells under hypoxia. (E and F) qRT-PCR (E) and western blotting (F) showing IL-33 expression levels under hypoxia in NM11 cells treated with HIF inhibitors. Cells were cultured under the same conditions as in Fig. 1 G and H. (G and H) qRT-PCR (G) and western blot (H) showing IL-33 levels in NM11 cells treated with HIF1- $\alpha$  activators. Cells were cultured under the same conditions as in Fig. 1 I and J. All data are presented as the mean  $\pm$  SD of biologically independent samples ( $n = 3$ ).  $P$  values were analyzed by one-way ANOVA with Bonferroni correction for multiple comparisons for C, E, and G. \*\*\*\* $P < 0.0001$ ; \*\*\*\* $P < 0.001$ ; ns, not significant. The uncropped western blot images are shown in [SI Appendix](#).

interactions between IL-33 and GATA3. Under hypoxia, IL-33 mRNA and nuclear protein levels were increased while those of GATA3 remained constant (Fig. 4 A and B). Immunofluorescence staining showed that GATA3 localized to the nucleus regardless of the oxygen concentration, colocalizing with IL-33 under hypoxia (Fig. 4C). We also performed a pull-down assay using the Halo Tag-IL-33 fusion protein in HEK293 cells, which endogenously express GATA3 (52) ([SI Appendix](#), Fig. S8), and found that GATA3 and IL-33 interact only under hypoxia (Fig. 4D).

We therefore examined whether GATA3 is substantially involved in the regulation of sST2 expression in CRC cells. GATA3 siRNA depletion in NM11 cells reduced sST2 mRNA levels (Fig. 4E) and ST2 promoter activity (Fig. 4F), suggesting that GATA3 positively regulates sST2 expression. CHIP using an anti-GATA3 antibody showed that GATA3 bound predominantly to the ST2 proximal promoter rather than to the distal promoter. In addition, GATA3 occupancy was significantly reduced under hypoxia compared to under normoxia (Fig. 4G). Furthermore, the decreased GATA3 binding to the ST2 proximal promoter under hypoxia was restored by depletion of IL-33 (Fig. 4H) or HIF-1 $\alpha$  (Fig. 4I). To further corroborate these findings, we employed electrophoretic mobility shift assay (EMSA) analysis. The ST2 proximal promoter contains two potential GATA3 consensus sequences (WGATAR). The positions of these consensus sites from the transcription start site were -830 to -825 (5'-TTATCA-3') and

-742 to -737 (5'-TGATAG-3'). EMSA experiments were performed using the oligonucleotide probes -830 (-853/-814) and -742 (-765/-726), a negative control probe (NC) without the consensus sequence, as well as a positive control probe (PC) located within the MUC1 gene promoter (52). All probes except NC bound to recombinant GATA3 but not recombinant IL-33, as demonstrated by the formation of a DNA-protein complex. When an anti-GATA3 monoclonal antibody was introduced to the binding reaction, a supershifted complex was detected ([SI Appendix](#), Fig. S9 A and B). We also observed the presence of a shifted complex in experiments using the -830 probe and the nuclear extracts prepared from normoxic HEK293 cells expressing fil-33; this complex only decreased when the unlabeled -830 self-competitor was added in molar excess to suggest that the complex was likely a GATA3 consensus sequence-specific DNA-protein ligand, since there was no change in the presence of the mutated (mut) competitor ([SI Appendix](#), Fig. S9C). Although western blotting confirmed that nuclear extracts from normoxic and hypoxic cells contained equal levels of GATA3 ([SI Appendix](#), Fig. S9D), both the -830 and -742 probes showed reduced levels of the shifted complex in hypoxic nuclear extracts compared to normoxic extracts ([SI Appendix](#), Fig. S9E). In these experiments, we were unable to observe the clear formation of a supershifted complex with the addition of the anti-GATA3 antibody, although the reason was unclear. However, these results strongly suggest reduced

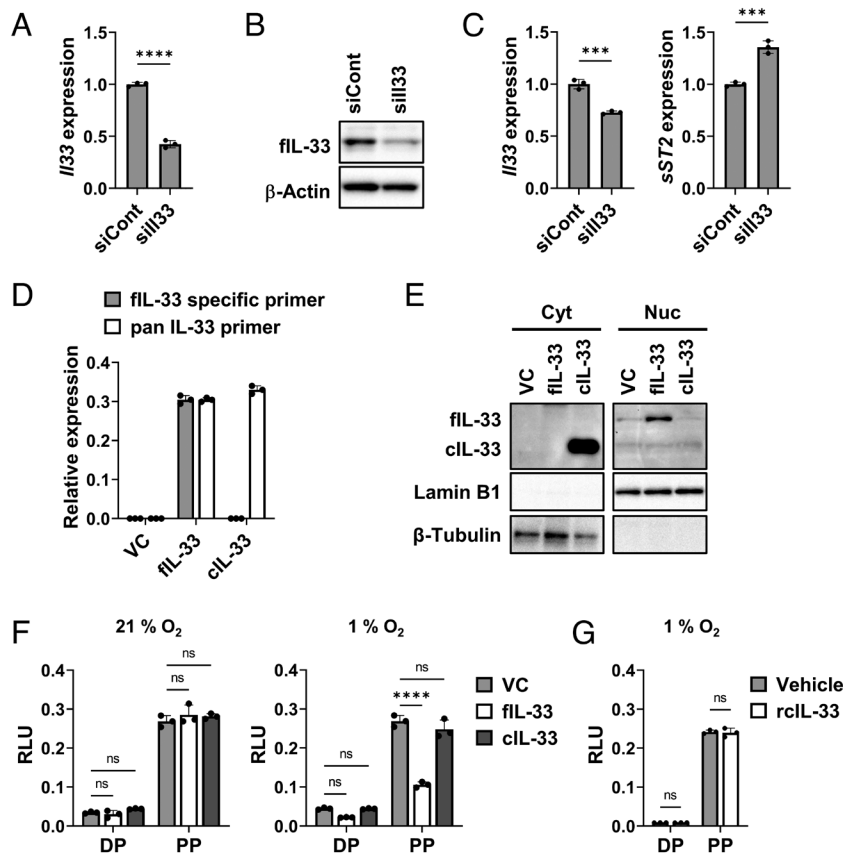


**Fig. 3.** ST2 gene promoter activity is repressed in a nuclear fIL-33-dependent manner under hypoxia. (A and B) qRT-PCR (A) and western blotting (B) showing siRNA-mediated IL-33 depletion in NM11 cells. (C) qRT-PCR analysis showing sST2 expression levels in IL-33-depleted NM11 cells under hypoxic condition (1% O<sub>2</sub>, 12 h). (D) qRT-PCR showing exogenous expression of human fIL-33 and/or cIL-33 in HEK293 cells. qPCR was performed using fIL-33-specific primers (detectable only for fIL-33) and pan IL-33 primers (detectable for cIL-33 and fIL-33). (E) Western blotting analysis showing protein expression and subcellular localization of exogenous fIL-33 and cIL-33 in HEK293 cells. (F and G) Dual-luciferase reporter assay. DP and PP indicate the distal and proximal ST2 promoters, respectively. (F) ST2 promoter activity under normoxic and hypoxic conditions in HEK293 cells expressing fIL-33 or cIL-33. (G) ST2 promoter activity in recombinant IL-33 (rcIL-33)-treated HEK293 cells. Cells were cultured in the presence of vehicle (DMSO) or 100 ng/mL rcIL-33 for 12 h under hypoxic conditions before the assay. All data are presented as the mean  $\pm$  SD of biologically independent samples ( $n = 3$ ).  $P$  values were analyzed by unpaired two-tailed  $t$  test for A, C, and G, and by one-way ANOVA with Bonferroni correction for multiple comparisons for F. \*\*\* $P < 0.001$ ; \*\*\*\* $P < 0.0001$ ; ns, not significant. The uncropped western blot images are shown in [SI Appendix](#).

GATA3 binding to the ST2 proximal promoter in hypoxic cells. Altogether, it is likely that under hypoxia, fIL-33 accumulates in the nucleus in a HIF-dependent manner and binds to GATA3, thereby blocking GATA3 access to the ST2 promoter and interfering with ST2 gene transcription. In this context, gene set enrichment analysis using the microarray gene expression data from IL-33-expressing HEK293 cells showed a trend toward altered expression levels of GATA3 target genes under hypoxia ([SI Appendix](#), Fig. S10). Incidentally, exogenous IL-33 expression and hypoxia did not affect endogenous GATA3 expression in HEK293 cells.

**sST2 Expression Is Reduced in the Hypoxic Regions of Human and Mouse CRC Tumors.** To examine whether sST2 expression is down-regulated in hypoxic tumor cells in vivo, immunofluorescence staining for sST2 was performed in the hypoxic regions of NM11 tumors. Since there are no antibodies that distinguish ST2 isoforms, an anti-ST2 antibody that recognizes both ST2L and sST2 was used. Double immunofluorescence staining with this antibody and an antibody against the hypoxia-detecting agent pimonidazole revealed that ST2 levels tended to decrease in hypoxic tumor regions (Fig. 5A). We subsequently determined whether the ST2 suppression in hypoxic regions actually occurs in tumor cells. To this end, we generated 5HRE/GFP-NM11 cells by introducing a hypoxia-responsive element (HRE)-regulated GFP

expression plasmid (5HRE/GFP) into NM11 cells ([SI Appendix](#), Fig. S11) and subcutaneously transplanted these cells into mice to establish tumors. The results showed a perfect coincidence between GFP-positive and pimonidazole-positive regions in the tumors, confirming hypoxia-induced GFP expression in tumor cells in vivo. ST2 immunostaining of these tumor sections revealed decreased ST2 levels in GFP-positive hypoxic tumor cells (Fig. 5B). We further investigated the relationship between the hypoxic tumor microenvironment and ST2 expression in human CRC lesions. Immunofluorescence staining of HIF-1 $\alpha$  and ST2 using human CRC tissue microarrays revealed that their expression in primary CRC lesions was inversely correlated. Furthermore, staining with an anti-IL-33 antibody confirmed the IL-33 and HIF-1 $\alpha$  colocalization. The same trend was more pronounced in CRC metastatic lesions in the lungs (Fig. 5C and [SI Appendix](#), Fig. S12). In contrast, in normal colon tissue, ST2 was strongly expressed in intestinal epithelial cells, but HIF-1 $\alpha$  and IL-33 positivity was barely detectable (Fig. 5C and [SI Appendix](#), Fig. S12). These results suggest that the pattern of ST2 expression differs between CRC lesions and normal tissue. Its expression tends to decrease in hypoxic regions and is inversely correlated with IL-33 expression. The significantly higher percentage of HIF-1 $\alpha$ -positive hypoxic cells in CRC lesions compared to normal colon tissue suggests that the decreased sST2 expression in hypoxic tumor cells may affect CRC pathogenesis (Fig. 5D).

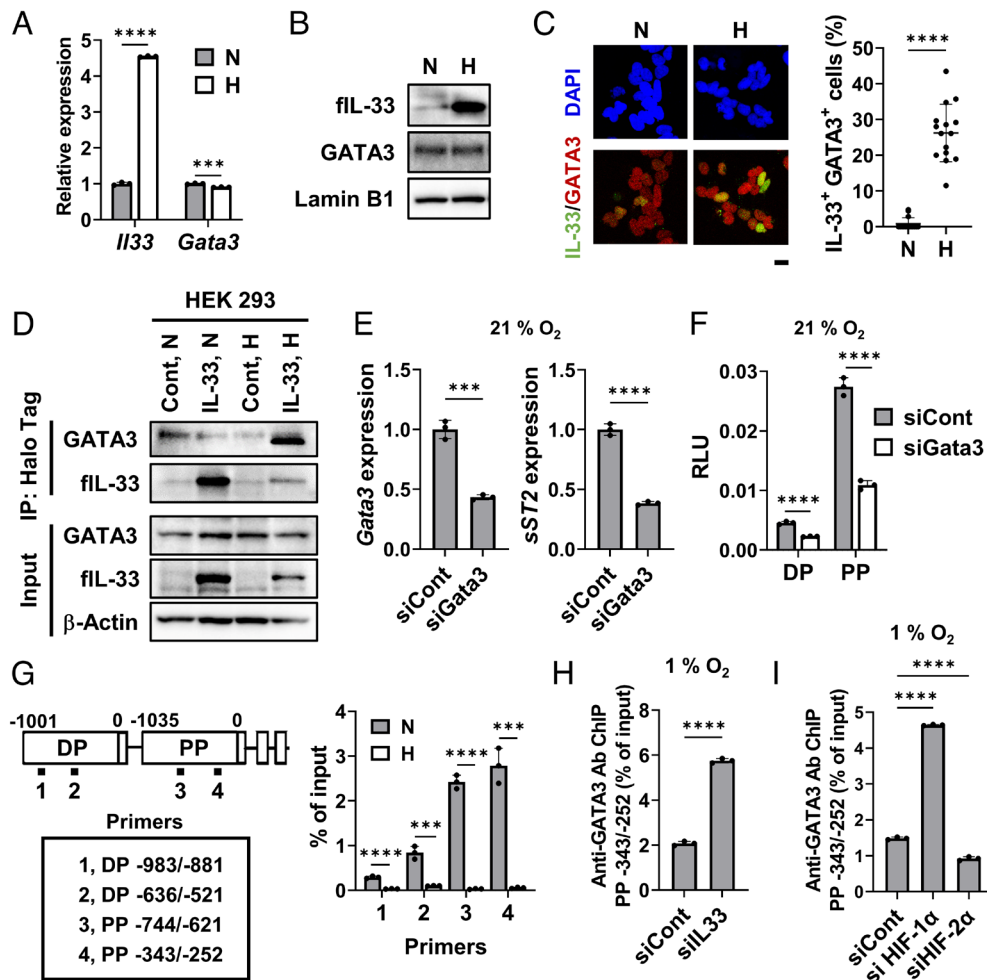


**Fig. 4.** Nuclear IL-33 binds to GATA3 under hypoxia and blocks GATA3 access to the ST2 promoter. (A and B) Expression status of GATA3 in NM11 cells under normoxic (N, 21% O<sub>2</sub> 12 h) or hypoxic (H, 1% O<sub>2</sub> 12 h) conditions. qRT-PCR analysis showing GATA3 mRNA levels (A) and western blotting analysis showing GATA3 protein levels in nuclear fractions (B). (C) Representative immunofluorescence staining images showing subcellular distribution of GATA3 and IL-33 in SW480 cells. Cells were cultured under normoxic (N, 21% O<sub>2</sub> 12 h) or hypoxic (H, 1% O<sub>2</sub> 12 h) conditions. (Scale bar, 20 μm.) Three pictures were acquired for each condition, five locations were randomly selected per image, and the percentage of IL-33<sup>+</sup> GATA3<sup>+</sup> cells was calculated. *n* = 15. (D) HaloTag pull-down assay showing protein–protein interactions between fil-33 and GATA3 in HEK293 cells under hypoxia. (E) qRT-PCR showing sST2 mRNA levels in GATA3-depleted SW480 cells. (F) Dual-luciferase reporter assay showing distal (DP) and proximal promoter (PP) activity in GATA3-depleted SW480 cells under normoxic conditions (21% O<sub>2</sub> 12 h). (G) ChIP-qPCR showing GATA3 occupancy on human ST2 promoters. Chromatin samples from SW480 cells immunoprecipitated with anti-GATA3 antibody subjected to qPCR using the four primer sets indicated on the left. (H and I) ChIP-qPCR showing GATA3 occupancy on the proximal promoter in IL-33-depleted (H) or HIF-depleted (I) SW480 cells. Data of A, B, and E–I are presented as the mean ± SD of biologically independent samples. *P* values were analyzed by unpaired two-tailed *t* test for A, C, and E–H and by one-way ANOVA with Bonferroni correction for multiple comparisons for I. \*\*\*\**P* < 0.001; \*\*\*\**P* < 0.0001. The uncropped western blot images are shown in *SI Appendix*.

### Restoration of sST2 Expression in the Hypoxic Regions of CRC Tumors Suppresses Tumor Growth.

Next, to determine whether reduced sST2 expression in the hypoxic regions of CRC tumors affects tumor growth, a hypoxia-responsive sST2 expression vector with five HREs was constructed and transfected into NM11 cells to obtain 5HRE/sST2-NM11#3 cells (hereafter, sST2-NM11) that express sST2 under hypoxia as under normoxia. Vector control cells, designated 5HRE/cont-NM11#3 (hereafter, Cont-NM11), were also established (*SI Appendix*, Fig. S13 A–C). Hypoxic culture slightly inhibited proliferation of both cells, but there were no signs of cell death (*SI Appendix*, Fig. S13 D–F). To assess tumor growth, these cells were subcutaneously transplanted into mice. The volume and weight of sST2-NM11 tumors were significantly lower than those of Cont-NM11 tumors (Fig. 6A and *SI Appendix*, Fig. S14 A–C). Consistent with this finding, sST2-NM11 tumors had fewer Ki67-positive cells than Cont-NM11 tumors, indicating that tumor growth was suppressed (Fig. 6B). No serious adverse effects such as weight loss were observed in sST2-NM11 tumor-bearing mice (*SI Appendix*, Fig. S14D). Whole-tumor sST2 mRNA

levels were significantly higher in sST2-NM11 tumors than those in Cont-NM11 tumors, without affecting ST2L and IL-33 levels (Fig. 6C and *SI Appendix*, Fig. S14E). Immunofluorescence staining showed that ST2 levels were lower in hypoxic regions than those in nonhypoxic regions in Cont-NM11 tumors but were comparable in both regions in sST2-NM11 tumors (Fig. 6D). Although it is difficult to distinguish membrane-bound ST2L from sST2 by immunofluorescence staining, most ST2 protein in tumors detected by western blotting was sST2, suggesting that the ST2 signal observed in the tumor tissue primarily reflects sST2 rather than ST2L (Fig. 6E). In addition, ELISA measurements showed significantly higher sST2 concentrations in protein extracts from tumors in sST2-NM11 tumors than those in Cont-NM11 tumors, while serum sST2 levels did not differ between groups (Fig. 6F and *SI Appendix*, Fig. S14F). These data indicate that sST2 expression was restored in the hypoxic regions of sST2-NM11 tumors, an effect that appears to be limited to tumor tissue.

In CRC tumors, sST2 modulates the inflammatory microenvironment by inhibiting IL-33/ST2L-mediated tumor-associated

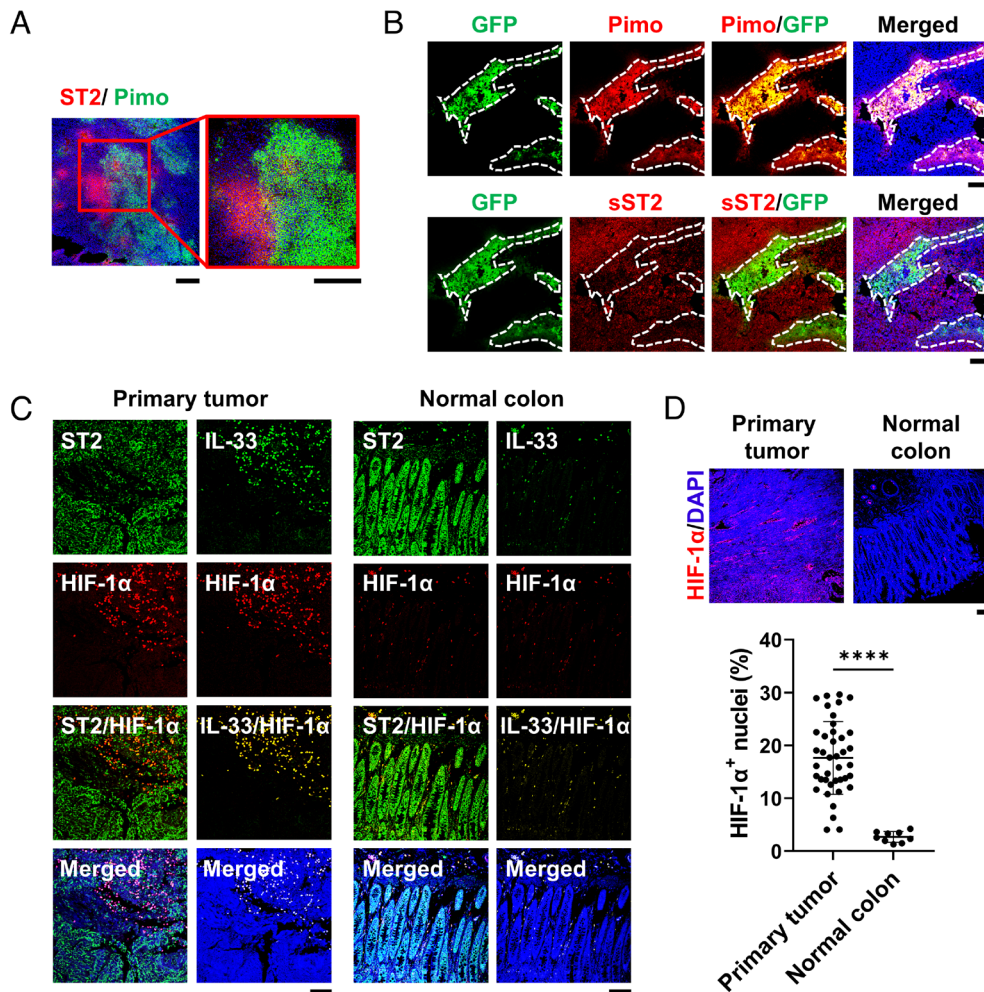


**Fig. 5.** Hypoxic regions of CRC tumors show decreased ST2 expression and increased IL-33 expression. (A) Representative images of immunofluorescence staining showing pimonidazole-positive hypoxic regions (Pimo, green) and ST2-expressing cells (red) in NM11 tumor sections. A magnified view of the boxed area is shown below. (Scale bars, 200  $\mu\text{m}$ .) (B) Representative images of immunofluorescence staining showing the relationship between hypoxia-induced GFP-expressing tumor cells (green) and pimonidazole-positive hypoxic regions (Pimo, red, surrounded by white dotted lines) or ST2-positive cells (green) in NM11 tumor sections. The inside of the white dotted line indicates the hypoxic region. (Scale bars, 100  $\mu\text{m}$ .) (C) Representative images of immunofluorescence staining showing the distribution of HIF-1 $\alpha$  (red), ST2 (green), or IL-33 (green) in tissue microarrays from CRC patients. (Scale bars, 50  $\mu\text{m}$ .) Nuclear counterstaining with DAPI was performed in all immunofluorescence staining. (D) Percentages of hypoxic cells in the tissue. Using the same tissue microarray as in C, the numbers of hypoxic cell nuclei (HIF-1 $\alpha$  positive) and total nuclei were counted in sections of CRC primary tumors ( $n = 40$ ) and adjacent normal tissue ( $n = 9$ ). (Scale bar, 100  $\mu\text{m}$ .) Data in D are presented as the mean  $\pm$  SD.  $P$  value was analyzed by unpaired two-tailed  $t$  test. \*\*\*\* $p < 0.0001$ .

macrophage mobilization, angiogenesis, and Th2 differentiation, generating a tumor-suppressive state (32). Therefore, we investigated the effect of restoring sST2 expression in the hypoxic region of the tumors on these bioprocesses. Immunofluorescence staining for CD31 and F4/80 revealed significantly reduced vascular density and macrophage infiltration in sST2-NM11 tumors compared to Cont-NM11 tumors (Fig. 6 G and H). In addition, PCR array analysis of Th1/Th2-related gene expression in tumor tissues suggested that sST2-NM11 tumors had lower Th2 cytokine and chemokine expression than 5HRE/cont-NM11 tumors (SI Appendix, Fig. S15A). Consistent with these findings, qRT-PCR indicated that sST2-NM11 tumors tended to express higher Th1-related genes (*Ccl5* and *Cxcr3*) and lower Th2-related genes (*Ccl7*, *Cebpb*, *Il6*, and *Il7*; SI Appendix, Fig. S15B). We also investigated the effect on M2 macrophage differentiation, which is closely related to the Th2 phenotype, and found that the expression of M2 markers, such as arginase and CD163, was significantly lower in sST2-NM11 tumors than that in Cont-NM11 tumors (Fig. 6I). In addition, because CD4 and Treg cells are the dominant effector cells of IL-33 (22, 53), we investigated the status of these cell populations in sST2-expressing and nonexpressing tumors by

double immunofluorescence staining using anti-CD4 and anti-FOXP3 antibodies. We found that not only the number of CD4 cells but also the percentage of CD4<sup>+</sup>FOXP3<sup>+</sup> Treg cells was decreased in sST2-NM11 tumors compared to Cont-NM11 tumors (Fig. 6J and SI Appendix, Fig. S16). Taken together, these results suggest that restoring sST2 expression in CRC cells in hypoxic tumor regions may modulate the inflammatory microenvironment and lead to tumor suppression.

**Restoration of sST2 Expression Confined to Hypoxic Regions of CRC Tumors Inhibits Metastasis.** NM11 cells are not suitable for assessing metastasis due to their low metastatic potential. Therefore, we used LuM1 cells, a counterpart of NM11 cells with high metastatic potential and low sST2 expression, to examine the effect of restoring sST2 expression in hypoxic tumor cells on metastasis. To this end, LuM1 cells expressing sST2 in response to hypoxia were prepared in the same manner as NM11 cells. Among the stable clones, cells showing similar levels of sST2 expression under hypoxia and normoxia (5HRE/sST2-LuM1#1 cells, hereafter termed sST2-LuM1#1) and cells showing higher sST2 expression under hypoxia than that under normoxia (5HRE/sST2-LuM1#21

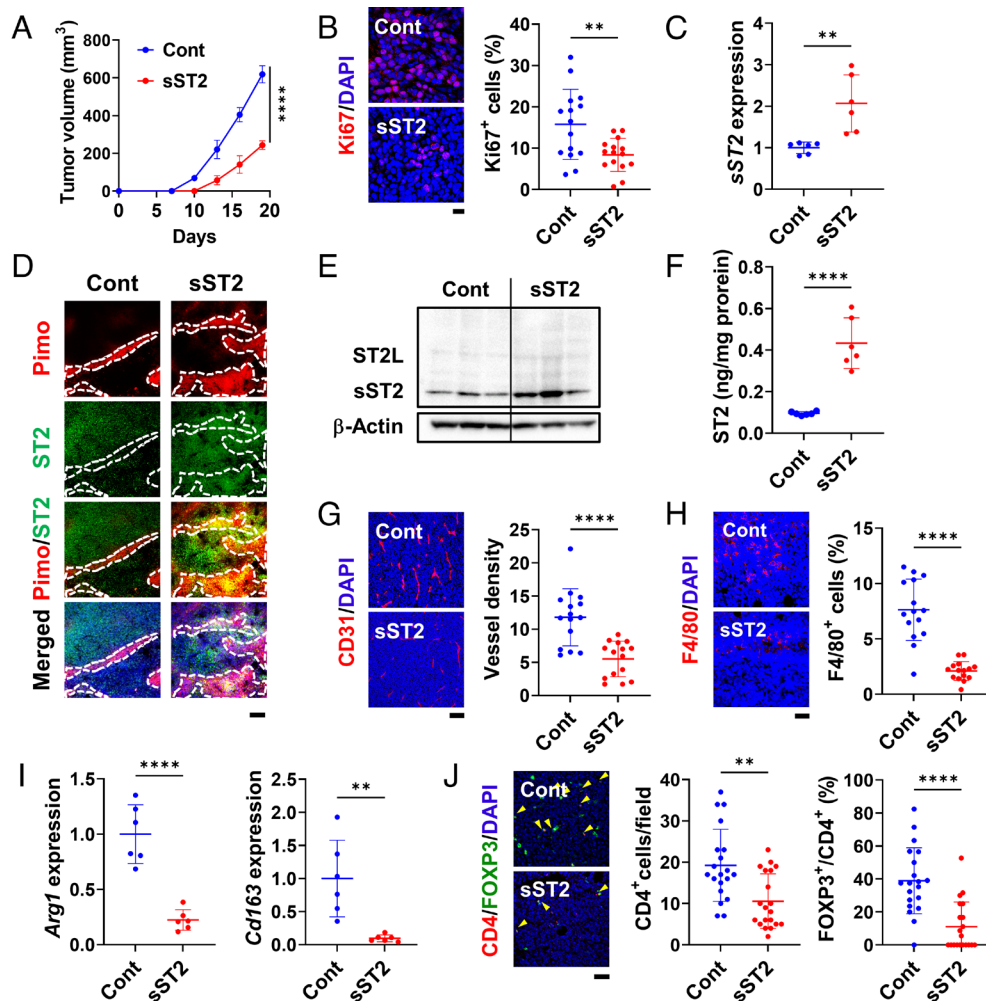


**Fig. 6.** Hypoxia-responsive sST2 expression in mouse CRC cells suppresses tumor growth and modifies the inflammatory microenvironment. (A) Effect of hypoxia-responsive sST2 expression in NM11 cells on tumor growth. Tumor size was measured every 3 d from day 7 after implantation after formation of palpable tumors ( $n = 6$  per group). Tumor volumes on day 19 were statistically compared. (B) Representative images of immunofluorescence staining of Ki67-positive proliferating cells in tumor tissues. (Scale bar, 20  $\mu\text{m}$ .) The percentage of Ki67<sup>+</sup> cells was calculated for each image ( $n = 15$  per group). (C) qRT-PCR showing sST2 levels in whole-tumor tissues ( $n = 6$  per group). (D) Representative images of immunofluorescence staining presenting ST2 expression (green) and pimonidazole-positive hypoxic region (Pimo, red, surrounded by white dotted lines) in the tumor tissues. (Scale bar, 100  $\mu\text{m}$ .) (E) Representative images of western blotting showing sST2 protein levels in whole-tumor tissues. (F) ELISA analysis showing sST2 concentrations in protein extracts from whole tumors ( $n = 6$  per group). (G) Representative images of immunofluorescence staining of CD31-positive vascular endothelial cells in tumor tissues. (Scale bar, 100  $\mu\text{m}$ .) The vessel density in each image was quantified using ImageJ software ( $n = 15$  per group). (H) Representative images of immunofluorescence staining showing macrophage infiltration into tumors. (Scale bar, 50  $\mu\text{m}$ .) The percentage of F4/80<sup>+</sup> cells was calculated for each image ( $n = 15$  per group). (I) qRT-PCR showing M2 marker expression in whole-tumor tissues ( $n = 6$  per group). (J) Representative images of immunofluorescence staining showing helper T (CD4<sup>+</sup>) and Treg (CD4<sup>+</sup> FOXP3<sup>+</sup>) cells in the tumor. CD4 is presented in green, FOXP3 in red, and nuclear counterstaining with DAPI in blue. Arrowheads indicate CD4<sup>+</sup>FOXP3<sup>+</sup> cells. (Scale bar, 50  $\mu\text{m}$ .) Enlarged versions of these images are shown in *SI Appendix, Fig. S16*. The numbers of CD4<sup>+</sup> cells and CD4<sup>+</sup>FOXP3<sup>+</sup> cells were counted and quantified for each image ( $n = 20$  per group). The data of A–C and F–J are presented as the mean  $\pm$  SD of biologically independent samples. *P* values were analyzed by unpaired two-tailed *t* test. \*\**P* < 0.01; \*\*\*\**P* < 0.0001. The uncropped western blot images are shown in *SI Appendix*.

cells, hereafter termed sST2-LuM1#21) were selected (*SI Appendix, Fig. S17 A–C*). In hypoxic culture conditions, proliferation was suppressed in all cell lines, including vector control cells (5HRE/cont-LuM1#3 cells, hereafter termed Cont-LuM1), regardless of hypoxic-responsive sST2 expression; in any case, cell viability was not affected (*SI Appendix, Fig. S17 D–F*). When these cells were transplanted subcutaneously into mice, the growth of sST2-LuM1#1 and sST2-LuM1#21 tumors was suppressed without weight loss compared to Cont-LuM1 tumors (Fig. 7*A* and *SI Appendix, Fig. S18 A–D*). In particular, marked growth inhibition was observed in sST2-LuM1#21 tumors with a decrease in Ki67-positive cells (Fig. 7*B*). sST2 mRNA levels were significantly higher in sST2-LuM1 tumors than those in Cont-LuM1 tumors; sST2-LuM1#21 tumors in particular were highly noticeable (Fig. 7*C*). ST2 (probably sST2) expression in the hypoxic regions was also higher in sST2-LuM1 tumors than that

in Cont-LuM1 tumors (Fig. 7*D*). The expression levels of ST2L and IL-33 showed little to no difference (*SI Appendix, Fig. S18E*). Serum concentrations of sST2 were comparable in all tumor-bearing mice (*SI Appendix, Fig. S18F*), whereas tumor extracts exhibited higher levels in the order of Cont<#1<#21 tumors (Fig. 7*E* and *F*). Similar to NM11 tumors, hypoxia-responsive sST2 expression in LuM1 tumors was associated with decreased tumor vascular density, macrophage infiltration, Th2-related gene expression, and the number of CD4 cells. In particular, the percentage of Treg cells was markedly reduced in tumor #21 (Fig. 7*G–I* and *SI Appendix, Fig. S15B*).

Intriguingly, the total number of metastatic nodules on the lung surface of mice with sST2-LuM1#21 tumors was significantly lower than that of mice with control tumors. Notably, sST2-LuM1#1 mice had significantly fewer large nodules (>0.05 mm), even though the total number of metastatic nodules was comparable to



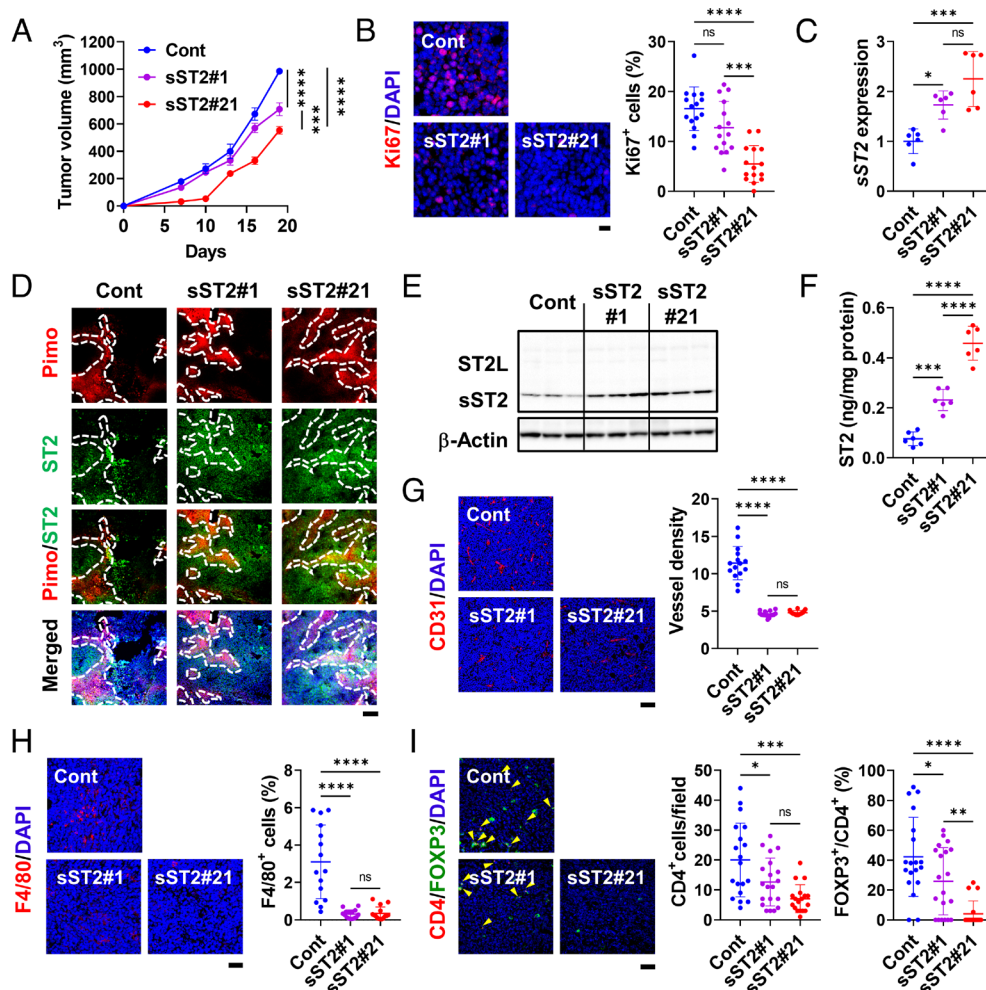


**Fig. 7.** Hypoxia-responsive sST2 expression in highly metastatic mouse CRC cells suppresses tumor growth. (A) Effect of hypoxia-responsive sST2 expression in LuM1 cells on tumor growth. Tumor size was measured every 3 d from day 7 after implantation after formation of palpable tumors ( $n = 6$  per group). Tumor volumes on day 19 were statistically compared. (B) Representative images of immunofluorescence staining of Ki67-positive proliferating cells in tumor tissues. (Scale bar, 20  $\mu\text{m}$ .) The percentage of Ki67<sup>+</sup> cells was calculated for each image ( $n = 15$  per group). (C) qRT-PCR showing sST2 expression in whole-tumor tissues ( $n = 6$  per group). (D) Representative images of immunofluorescence staining presenting ST2 expression (green) and pimonidazole-positive hypoxic region (Pimo, red, surrounded by white dotted lines) in the tumor tissues. (Scale bar, 100  $\mu\text{m}$ .) (E) Representative images of western blotting showing sST2 protein levels in whole-tumor tissues. (F) ELISA analysis showing sST2 concentrations in protein extracts from whole tumors ( $n = 6$  per group). (G) Representative images of immunofluorescence staining of CD31-positive vascular endothelial cells in tumor tissues. (Scale bar, 100  $\mu\text{m}$ .) Vessel density in each image was quantified using ImageJ software ( $n = 15$  per group). (H) Representative images of immunofluorescence staining showing macrophage infiltration into tumors. (Scale bar, 50  $\mu\text{m}$ .) The percentage of F4/80<sup>+</sup> cells was calculated for each image ( $n = 15$  per group). (I) Representative images of immunofluorescence staining presenting helper T (CD4<sup>+</sup>) and Treg (CD4<sup>+</sup> FOXP3<sup>+</sup>) cells in the tumor. CD4 is presented in green, FOXP3 in red, and nuclear counterstaining with DAPI in blue. Arrowheads indicate CD4<sup>+</sup>FOXP3<sup>+</sup> cells. (Scale bar, 50  $\mu\text{m}$ .) Enlarged versions of these images are shown in *SI Appendix*, Fig. S16. The numbers of CD4<sup>+</sup> cells and CD4<sup>+</sup>FOXP3<sup>+</sup> cells were counted and quantified for each image ( $n = 20$  per group). Data in A–C and F–I are presented as the mean  $\pm$  SD of biologically independent samples. *P* values were analyzed by one-way ANOVA with Bonferroni correction for multiple comparisons. \* $P < 0.05$ ; \*\* $P < 0.01$ ; \*\*\* $P < 0.001$ ; \*\*\*\* $P < 0.0001$ ; ns, not significant. The uncropped western blot images are shown in *SI Appendix*.

that of control mice (Fig. 8 *A* and *B*). Furthermore, hematoxylin–eosin staining of lung tissue revealed that the number of micrometastases per section significantly decreased with increasing hypoxia-responsive sST2 expression in LuM1 cells (Fig. 8 *C* and *D*). These results suggest that hypoxia-responsive sST2 expression in highly metastatic CRC cells inhibits tumor growth and lung metastasis.

## Discussion

This study demonstrates that hypoxia down-regulates sST2 expression in CRC cells via the HIF–IL-33–GATA3 axis. Under hypoxia, HIF-up-regulated IL-33 translocates to the nucleus and interacts with GATA3 to block its binding to the proximal promoter of the ST2 gene. Hypoxia-induced sST2 downregulation was also observed in the hypoxic regions of mouse and human CRC

tumors. Our most important finding was that restoring sST2 expression in the hypoxic regions of CRC tumors can alter the inflammatory tumor microenvironment and effectively suppress tumor growth and distant metastasis (*SI Appendix*, Fig. S19). Recently, it was shown that activation of nuclear IL-33/SMAD signaling in epithelial cells is important for the development of chronic inflammation-related cancers (54), and that nuclear IL-33 in Treg cells is essential for their immunosuppressive activity (31). In addition to these reports, the present study suggests that nuclear IL-33 has a significant impact on tumor malignancy.

To date, it has been reported that nuclear IL-33 directly binds to multiple homeoboxes in the distal and proximal promoters of the ST2 gene and recruits the methyltransferase SUV39H1 to promote histone H3K9 trimethylation (47). In our study, H3K9me3 levels at the ST2 distal and proximal promoters in CRC cells were only slightly increased in a time-dependent manner under hypoxia,

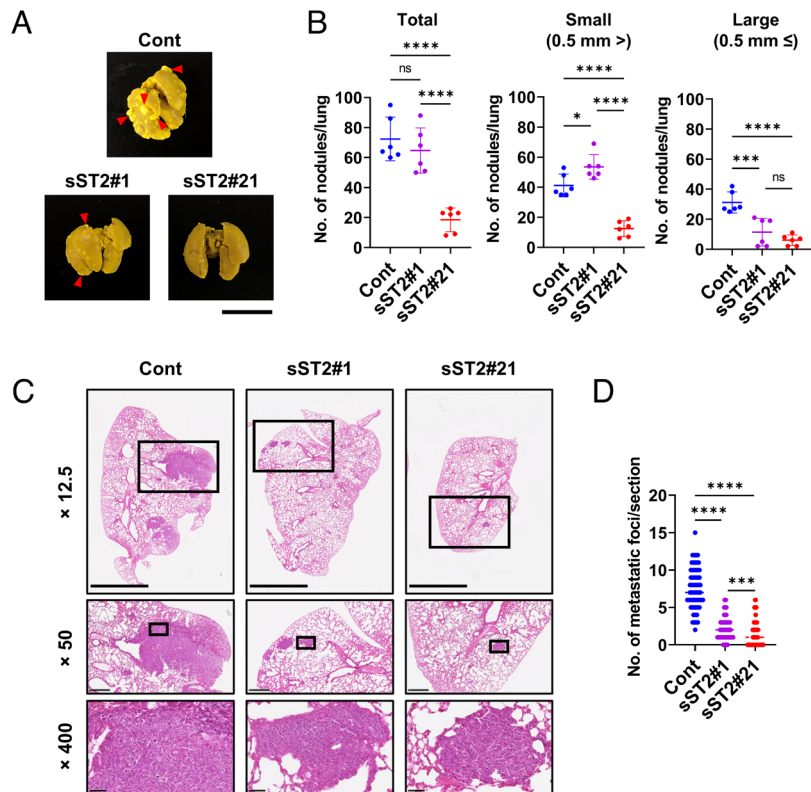


**Fig. 8.** Hypoxia-responsive sST2 expression in highly metastatic mouse CRC cells suppresses lung metastasis. (A) Representative macroscopic image of the lungs. Red arrowheads indicate metastatic nodules  $\geq 0.5$  mm in diameter. (Scale bar, 1 cm.) (B) Number of metastatic nodules per lung. In addition to the total number of nodules, large ( $\geq 0.5$  mm in diameter) and small ( $< 0.5$  mm in diameter) nodules are displayed separately. Data are presented as the mean  $\pm$  SD ( $n = 6$  in each group).  $P$  values were analyzed by one-way ANOVA adjusted for multiple comparisons. (C) Images of typical micrometastasis in hematoxylin- and eosin-stained sections of the left lung lobe. Scale bars indicate 2.5 mm at  $\times 12.5$  magnification, 500  $\mu$ m at  $\times 50$  magnification, and 50  $\mu$ m at  $\times 400$  magnification. (D) Number of metastatic nodules per section. Ten sections of 5 to 6 lungs per group were counted.  $P$  values were analyzed by the Mann-Whitney  $U$  test. \* $P < 0.05$ ; \*\*\* $P < 0.001$ ; \*\*\*\* $P < 0.0001$ ; ns, not significant.

an effect attenuated by IL-33 depletion, suggesting that IL-33 partially affects ST2 promoter activity under hypoxia via H3K9 trimethylation. Supporting this finding, treatment with chaetocin, an SUV39H1 inhibitor, did not fully restore sST2 expression under hypoxia. Therefore, we speculated that another mechanism is at work in hypoxic CRC cells to reduce sST2 expression: GATA3 binds to the proximal promoter of the ST2 gene, and nuclear IL-33 inhibited this binding. Thus, nuclear IL-33 in hypoxic cells acts as a transcriptional repressor of the ST2 gene. Similarly, nuclear IL-33 in IL-1 $\beta$ -stimulated cells tightly binds to the p65 subunit of NF- $\kappa$ B to form the IL-33/NF- $\kappa$ B complex, which inhibits NF- $\kappa$ B p65 binding to DNA and suppresses transcription and expression of NF- $\kappa$ B target genes such as I $\kappa$ B $\alpha$ , tumor necrosis factor (TNF)- $\alpha$ , and C-REL (51). On the contrary, nuclear IL-33 has been reported to bind directly to the promoter region of the NF- $\kappa$ B p65 subunit gene in response to TNF and acts as a transcriptional activator (55). As such, nuclear IL-33 may function as a transcriptional repressor or activator by binding to transcription factors, depending on cell types and cellular conditions. Another report showed that nuclear IL-33 forms a macromolecular complex with histones and is released extracellularly, binding to ST2L and synergistically activating IL-33/ST2L signaling (56). Thus, nuclear IL-33 can function as a transcriptional modulator in the nucleus and as an activator of ST2L signaling. Despite this knowledge, the function of nuclear IL-33 is not fully understood.

The hypoxia-specific interaction between IL-33 and GATA3 is not solely due to increased nuclear IL-33 levels. This is because although nuclear IL-33 levels were increased in HEK293 cells expressing exogenous IL-33 regardless of oxygen status, binding between nuclear IL-33 and GATA3 was only detected under

hypoxia. Therefore, some qualitative changes may occur in nuclear IL-33 under hypoxia. For example, in extracellular acidic environment, two disulfide bridges are formed within the IL-33 molecule, causing a large conformational change in the molecular structure and altering its binding ability to ST2 (57). Hypoxia/anoxia is reported to elevate intracellular pH (58). If hypoxia creates such acidic conditions in CRC cells, it is possible that conformational changes in nuclear IL-33 may occur that promote its binding to GATA3. Further studies are required to elucidate the mechanism underlying the IL-33–GATA3 interaction in hypoxia.

Hypoxia-responsive sST2 expression in CRC cells suppressed tumor growth and metastasis, although it did not affect cell proliferation in culture. As such, restoration of sST2 expression in hypoxic regions of tumors may shift the tumor microenvironment toward a tumor-suppressive state. Indeed, NM11 tumors expressing sST2 in response to hypoxia showed increased expression levels of the tumor-suppressive Th1-associated genes *Ccl5* and *Cxcr3* and decreased expression levels of the tumor-promoting Th2-associated genes *Ccl7*, *Cebpb*, *Il6*, and *Il7*. We previously demonstrated that systemic administration of recombinant sST2 to CRC tumor-bearing mice suppressed tumor growth and metastasis (32). However, this approach may be impractical due to the need for large amounts of recombinant protein to maintain high circulating sST2 levels and the risk of immune disorders resulting from imbalanced IL-33 and sST2 levels. In contrast, current data provide evidence that hypoxia-responsive elevation of sST2 levels is restricted to tumor tissue and can thus effectively suppress the growth and metastasis of CRC tumors without causing systemic adverse events. Therefore, strategies that block sST2 downregulation in hypoxic tumor regions appear to be able to suppress malignant CRC effectively and safely. One such strategy could

be the inhibition of HIFs, the most upstream regulators of sST2 expression in hypoxia. As a large number of small-molecule HIF inhibitors are under development (59), some may help maintain high sST2 levels in CRC tumors and ultimately treat high-grade CRC. Our report suggests that sST2 expression in CRC cells reduces tumor malignancy. However, the effects of sST2 may depend on cell type and context, i.e., sST2 exhibits tumor-promoting effects in gastric cancer (18), ER-positive breast cancer (30), and pancreatic cancer cells (60). Such discrepancies may be due to differences in inflammatory status in the microenvironment. Therefore, reduced sST2 expression in hypoxic regions of these tumors may have different implications and should be additionally investigated.

In conclusion, the present study described the linkage of HIF, nuclear IL-33, GATA3, and sST2 in hypoxia, which is closely associated with the malignant progression of CRC tumors. Recently, a relationship between the microenvironment and IL-33–ST2L signaling has been reported in various cancers (61). Accordingly, molecules involved in the IL-33–ST2L axis and sST2 in tumor tissue may be important targets to prevent the malignant progression of cancer. Further studies are warranted to evaluate this issue.

## Materials and Methods

**Cells and Cell Culture.** Mouse CRC NM11 cells and their highly metastatic counterparts LuM1 cells were established from the mouse colon adenocarcinoma Colo26 cell line (62). Human CRC SW480 cells and human fetal kidney HEK293 cells were obtained from ATCC. All cells were cultured in Dulbecco's Modified Eagle's Medium (Sigma-Aldrich, D6429) supplemented with 10% fetal bovine serum and 50 µg/mL gentamicin and maintained at 37 °C in a humidified atmosphere of 5% CO<sub>2</sub>. The cells were normally cultured at atmospheric oxygen concentrations (21%). Hypoxic cultures were performed in an atmosphere of 1% O<sub>2</sub>, 5% CO<sub>2</sub>, and 94% N<sub>2</sub> using a multigas incubator (Wakenyaku, 9000E). Alternatively, hypoxia mimetics such as CoCl<sub>2</sub>, DMOG, and DFO were added to the culture medium. For HIF-α inhibition under hypoxic conditions, cells were pretreated with the HIF-1α inhibitor SW6 or HIF-2α inhibitor TC-S 7009 for 12 h and exposed to 1% O<sub>2</sub>.

**RNA Preparation and qRT-PCR.** RNA preparation and qRT-PCR were conducted as previously described (32). Gene expression levels were normalized to beta-2 macroglobulin by the  $\Delta\Delta$ CT method. Primer information is detailed in *SI Appendix, Table S1*.

**siRNA-Mediated Gene Depletion.** MISSION® siRNAs (Sigma-Aldrich) specific for mouse *Hif1a*, *Hif2a*, *Il33*, and *Gata3* along with control siRNA were used. Each siRNA was transfected into cells using Lipofectamine® RNA iMAX Transfection Reagent (ThermoFisher Scientific, #13778075) according to the manufacturer's protocol.

**Western Blotting.** Western blotting was conducted as previously described (32). Information on the antibodies used in western blotting is presented in *SI Appendix, Table S2*. The uncropped images are shown in *SI Appendix*.

**ChIP-qPCR.** The information on ChIP-qPCR is provided in *SI Appendix*. The primers used are presented in *SI Appendix, Table S2*.

**Animal Experiments.** All animal experiments were performed according to the guidelines of the Institutional Review Board (19-008) of Teikyo University. The information on tumor transplantation is provided in *SI Appendix*.

**HaloTag Pull-Down Assay.** The information on HaloTag pull-down assay is provided in *SI Appendix*. Antibodies used in this experiment are presented in *SI Appendix, Table S3*.

**Immunohistochemistry.** Frozen tumor sections (10 µm thick) were prepared using a cryostat (Leica, CM3050). Immunohistochemistry was conducted as previously described (32). Anti-pimonidazole antibody and the secondary antibody included in the Hypoxyprobe™-1 kit (Hypoxyprobe, HP1-100) were used to detect hypoxic regions. All antibodies used in this experiment are presented in *SI Appendix, Table S3*.

**Detection of Pulmonary Micrometastases.** The left lungs were fixed with formaldehyde, embedded in paraffin, and cut into 5-µm sections. Ten sections at 50 µm intervals in each lung lobe were prepared for staining with hematoxylin and eosin. Metastatic foci were counted under a bright field microscope.

**Tissue Microarray Staining.** The information on tissue microarray staining is provided in *SI Appendix*. All antibodies used in this experiment are presented in *SI Appendix, Table S3*.

**Luciferase Reporter Assay.** The information on the luciferase reporter assay is provided in *SI Appendix*.

**ELISA.** The information on ELISA is provided in *SI Appendix*.

**Preparation of Hypoxia-Induced Expression Vectors and Transfection.** The information on preparation of hypoxia-induced expression vectors and transfection is provided in *SI Appendix*.

**Microarray Analysis.** The information on microarray analysis is provided in *SI Appendix*.

**PCR Array.** RT<sup>2</sup> Profiler™ PCR Array Mouse Th1 & Th2 Responses (Qiagen, #330231) were used to screen for Th1/Th2 cytokine expression in tumor tissue. Using the total RNA extracted from the tumor, reverse transcription followed by qPCR was performed as previously described (32). Data were analyzed using the web analysis tool for PCR arrays provided by Qiagen.

**EMSA.** The information on EMSA is provided in *SI Appendix*. All probes used in this experiment are presented in *SI Appendix, Table S4*.

**Statistical Analysis.** Statistical analysis was performed using GraphPad Prism 9 software (GraphPad). All data were expressed as the mean ± SD. Statistical significance between two datasets was evaluated using an unpaired two-tailed *t* test. We used one-way ANOVA with Bonferroni correction to compare data from multiple groups. To evaluate the difference in the number of metastatic nodules in hematoxylin- and eosin-stained tissue sections, we used a Mann-Whitney *U* test. *P* < 0.05 was considered statistically significant.

**Data, Materials, and Software Availability.** All study data are included in the article and/or *SI Appendix*.

**ACKNOWLEDGMENTS.** This work was supported by JSPS KAKENHI Grant Numbers 16K21177, 19K07673, and 22K07217 to M.A.; 19K07654 to K.T.; and 19K11651 to M.T.-A. We would like to thank Enago ([www.enago.jp](http://www.enago.jp)) for the English language review.

---

Author affiliations: <sup>a</sup>Department of Biochemistry, Teikyo University School of Medicine, Kaga, Itabashi-ku, Tokyo 173-8605, Japan; <sup>b</sup>Department of Innovative Cancer Therapeutics, Chiba Cancer Center Research Institute, Nitona, Chuoh-ku, Chiba 260-8717, Japan; <sup>c</sup>Medical Education Center, Teikyo University School of Medicine, Kaga, Itabashi-ku, Tokyo 173-8605, Japan; and <sup>d</sup>Department of Internal Medicine, Teikyo University School of Medicine, Kaga, Itabashi-ku, Tokyo 173-8605, Japan

Author contributions: M.A. designed research; M.A., T.S., N.O., N.K., H.H., and K.T. performed research; M.A., T.S., N.O., N.K., H.H., and K.T. analyzed data; H.O. supervision; M.I., K.T., T.O., and M.T.-A. supervision, writing-review and editing; and M.A., K.T., T.O., and M.T.-A. wrote the paper.

1. H. Sung *et al.*, Global cancer statistics 2020: GLOBOCAN estimates of incidence and mortality worldwide for 36 cancers in 185 countries. *CA Cancer J. Clin.* **71**, 209–249 (2021).
2. J. Schmitz *et al.*, IL-33, an interleukin-1-like cytokine that signals via the IL-1 receptor-related protein ST2 and induces T helper type 2-associated cytokines. *Immunity* **23**, 479–490 (2005).
3. D. Bertheloot, E. Latz, HMGB1, IL-1α, IL-33 and S100 proteins: Dual-function alarmins. *Cell. Mol. Immunol.* **14**, 43–64 (2017).
4. H. Hayakawa, M. Hayakawa, A. Kume, S. I. Tominaga, Soluble ST2 blocks interleukin-33 signaling in allergic airway inflammation. *J. Biol. Chem.* **282**, 26369–26380 (2007).

5. M. De la Fuente, T. T. MacDonald, M. A. Hermoso, The IL-33/ST2 axis: Role in health and disease. *Cytokine Growth Factor Rev.* **26**, 615–623 (2015).
6. Y. Imai, Interleukin-33 in atopic dermatitis. *J. Dermatol. Sci.* **96**, 2–7 (2019).
7. J. Zheng *et al.*, A novel function of NLRP3 independent of inflammasome as a key transcription factor of IL-33 in epithelial cells of atopic dermatitis. *Cell Death Dis.* **12**, 1–12 (2021).
8. D. Préfontaine *et al.*, Increased expression of IL-33 in severe asthma: Evidence of expression by airway smooth muscle cells. *J. Immunol.* **183**, 5094–5103 (2009).
9. R. J. Snelgrove *et al.*, Alternaria-derived serine protease activity drives IL-33-mediated asthma exacerbations. *J. Allergy Clin. Immunol.* **134**, 24–26 (2014).

10. E. D. Gordon *et al.*, Alternative splicing of interleukin-33 and type 2 inflammation in asthma. *Proc. Natl. Acad. Sci. U. S. A.* **113**, 8765–70 (2016).
11. W. A. Verri *et al.*, IL-33 induces neutrophil migration in rheumatoid arthritis and is a target of anti-TNF therapy. *Ann. Rheum. Dis.* **69**, 1697–703 (2010).
12. F. Hu *et al.*, Hypoxia-inducible factor-1 $\alpha$  and interleukin 33 form a regulatory circuit to perpetuate the inflammation in rheumatoid arthritis. *PLoS One* **8**, e72650 (2013).
13. C. Schiering *et al.*, The alarmin IL-33 promotes regulatory T-cell function in the intestine. *Nature* **513**, 564–568 (2014).
14. A. Waddell, J. E. Vallance, S. Fox, M. J. Rosen, IL-33 is produced by colon fibroblasts and differentially regulated in acute and chronic murine colitis. *Sci. Rep.* **11**, 1–11 (2021).
15. I. P. Jovanovic *et al.*, Interleukin-33/ST2 axis promotes breast cancer growth and metastases by facilitating intratumoral accumulation of immunosuppressive and innate lymphoid cells. *Int. J. Cancer* **134**, 1669–1682 (2014).
16. J. Liu, J. X. Shen, J. L. Hu, W. H. Huang, G. J. Zhang, Significance of interleukin-33 and its related cytokines in patients with breast cancers. *Front. Immunol.* **5**, 1–7 (2014).
17. P. Zhang *et al.*, Detection of interleukin-33 in serum and carcinoma tissue from patients with hepatocellular carcinoma and its clinical implications. *J. Int. Med. Res.* **40**, 1654–1661 (2012).
18. D. Bergis *et al.*, High serum levels of the interleukin-33 receptor soluble ST2 as a negative prognostic factor in hepatocellular carcinoma. *Transl. Oncol.* **6**, 311–318 (2013).
19. P. Sun *et al.*, Serum interleukin-33 levels in patients with gastric cancer. *Dig. Dis. Sci.* **56**, 3596–3601 (2011).
20. L.-A. Hu, Y. Fu, D.-N. Zhang, J. Zhang, Serum IL-33 as a diagnostic and prognostic marker in non-small cell lung cancer. *Asian Pac. J. Cancer Prev.* **14**, 2563–2566 (2013).
21. M. Akimoto, J.-I. Hayashi, S. Nakae, H. Saito, K. Takenaga, Interleukin-33 enhances programmed oncosis of ST2L-positive low-metastatic cells in the tumour microenvironment of lung cancer. *Cell Death Dis.* **7**, e2057 (2016).
22. E. Pastille *et al.*, The IL-33/ST2 pathway shapes the regulatory T cell phenotype to promote intestinal cancer. *Mucosal Immunol.* **12**, 990–1003 (2019).
23. R. L. Maywald *et al.*, IL-33 activates tumor stroma to promote intestinal polyposis. *Proc. Natl. Acad. Sci. U. S. A.* **112**, E2487–E2496 (2015).
24. G. Cui *et al.*, Dynamics of the IL-33/ST2 network in the progression of human colorectal adenoma to sporadic colorectal cancer. *Cancer Immunol. Immunother.* **64**, 181–190 (2015).
25. X. Liu *et al.*, IL-33/ST2 pathway contributes to metastasis of human colorectal cancer. *Biochem. Biophys. Res. Commun.* **453**, 486–492 (2014).
26. M. Akimoto, K. Takenaga, Role of the IL-33/ST2L axis in colorectal cancer progression. *Cell. Immunol.* **343**, 103740 (2019).
27. Y. Zhang *et al.*, IL-33 promotes growth and liver metastasis of colorectal cancer in mice by remodeling the tumor microenvironment and inducing angiogenesis. *Mol. Carcinog.* **56**, 272–287 (2016).
28. K. D. Mertz *et al.*, The IL-33/ST2 pathway contributes to intestinal tumorigenesis in humans and mice. *Oncotarget* **5**, e1062966 (2015).
29. M. M. Karimi *et al.*, A novel isoform of IL-33 revealed by screening for transposable element promoted genes in human colorectal cancer. *PLoS One* **12**, e0180659 (2017).
30. D. Lu *et al.*, Serum soluble ST2 is associated with ER-positive breast cancer. *BMC Cancer* **14**, 198 (2014).
31. A. Hatzioannou *et al.*, An intrinsic role of IL-33 in Treg cell-mediated tumor immunoevasion. *Nat. Immunol.* **21**, 75–85 (2020).
32. M. Akimoto, R. Maruyama, H. Takamaru, T. Ochiya, K. Takenaga, Soluble IL-33 receptor sST2 inhibits colorectal cancer malignant growth by modifying the tumour microenvironment. *Nat. Commun.* **7**, 1–15 (2016).
33. B. Muz, P. de la Puente, F. Azab, A. K. Azab, The role of hypoxia in cancer progression, angiogenesis, metastasis, and resistance to therapy. *Hypoxia* **3**, 83–92 (2015).
34. Q. Xiong *et al.*, Hypoxia and cancer related pathology. *Cancer Lett.* **486**, 1–7 (2020).
35. A. Sebestyén, L. Kopper, T. Dankó, J. Timár, Hypoxia signaling in cancer: From basics to clinical practice. *Pathol. Oncol. Res.* **27**, 1–15 (2021).
36. D. Triner, Y. M. Shah, Hypoxia-inducible factors: A central link between inflammation and cancer. *J. Clin. Invest.* **126**, 3689–3698 (2016).
37. L. D'Ignazio, M. Batie, S. Rocha, Hypoxia and inflammation in cancer, focus on HIF and NF- $\kappa$ B. *Biomedicines* **5**, 21 (2017).
38. G. Bergers, A. Reikerstorfer, S. Braselmann, P. Graninger, M. Busslinger, Alternative promoter usage of the Fos-responsive gene *Fit-1* generates mRNA isoforms coding for either secreted or membrane-bound proteins related to the IL-1 receptor. *EMBO J.* **13**, 1176–1188 (1994).
39. H. Iwahana *et al.*, Different promoter usage and multiple transcription initiation sites of the interleukin-1 receptor-related human ST2 gene in UT-7 and TM12 cells. *Eur. J. Biochem.* **264**, 397–406 (1999).
40. T. Gächter, A. K. Werenskiöld, R. Klemenz, Transcription of the interleukin-1 receptor-related T1 gene is initiated at different promoters in mast cells and fibroblasts. *J. Biol. Chem.* **271**, 124–129 (1996).
41. B. P. Lipsky, D. Y. Toy, D. A. Swart, M. D. Smithgall, D. Smith, Deletion of the ST2 proximal promoter disrupts fibroblast-specific expression but does not reduce the amount of soluble ST2 in circulation. *Eur. J. Immunol.* **42**, 1863–1869 (2012).
42. Y. Baba *et al.*, GATA2 is a critical transactivator for the human IL1RL1/ST2 promoter in mast cells/basophils. *J. Biol. Chem.* **287**, 32689–32696 (2012).
43. M. Hayakawa *et al.*, T-helper type 2 cell-specific expression of the ST2 gene is regulated by transcription factor GATA-3. *Biochim. Biophys. Acta Gene Struct. Expr.* **1728**, 53–64 (2005).
44. K. Tago *et al.*, STAT3 and ERK pathways are involved in cell growth stimulation of the ST2/IL1RL1 promoter. *FEBS Open Bio* **7**, 293–302 (2017).
45. L. Roussel, M. Erard, C. Cayrol, J.-P. Girard, Molecular mimicry between IL-33 and KSHV for attachment to chromatin through the H2A–H2B acidic pocket. *EMBO Rep.* **9**, 1006–1012 (2008).
46. V. Carriere *et al.*, IL-33, the IL-1-like cytokine ligand for ST2 receptor, is a chromatin-associated nuclear factor in vivo. *Proc. Natl. Acad. Sci. U. S. A.* **104**, 282–287 (2007).
47. D. Shao *et al.*, Nuclear IL-33 regulates soluble ST2 receptor and IL-6 expression in primary human arterial endothelial cells and is decreased in idiopathic pulmonary arterial hypertension. *Biochem. Biophys. Res. Commun.* **451**, 8–14 (2014).
48. K. Lee *et al.*, LW6, a novel HIF-1 inhibitor, promotes proteasomal degradation of HIF-1 $\alpha$  via upregulation of VHL in a colon cancer cell line. *Biochem. Pharmacol.* **80**, 982–989 (2010).
49. T. Sasagawa *et al.*, HIF-2 $\alpha$ , but not HIF-1 $\alpha$ , mediates hypoxia-induced up-regulation of Flt-1 gene expression in placental trophoblasts. *Sci. Rep.* **8**, 1–13 (2018).
50. M. Sun *et al.*, Hypoxia inducible factor-1 $\alpha$ -induced interleukin-33 expression in intestinal epithelia contributes to mucosal homeostasis in inflammatory bowel disease. *Clin. Exp. Immunol.* **187**, 428–440 (2017).
51. S. Ali *et al.*, The dual function cytokine IL-33 interacts with the transcription factor NF- $\kappa$ B to dampen NF- $\kappa$ B-stimulated gene transcription. *J. Immunol.* **187**, 1609–1616 (2011).
52. M. C. Abba *et al.*, GATA3 protein as a MUC1 transcriptional regulator in breast cancer cells. *Breast Cancer Res.* **8**, 1–11 (2006).
53. A. H. Ameri *et al.*, IL-33/regulatory T cell axis triggers the development of a tumor-promoting immune environment in chronic inflammation. *Proc. Natl. Acad. Sci. U. S. A.* **116**, 2646–2651 (2019).
54. J. H. Park *et al.*, Nuclear IL-33/SMAD signaling axis promotes cancer development in chronic inflammation. *EMBO J.* **40**, 1–16 (2021).
55. Y. S. Choi *et al.*, Nuclear IL-33 is a transcriptional regulator of NF- $\kappa$ B p65 and induces endothelial cell activation. *Biochem. Biophys. Res. Commun.* **421**, 305–311 (2012).
56. J. Travers *et al.*, Chromatin regulates IL-33 release and extracellular cytokine activity. *Nat. Commun.* **9**, 1–15 (2018).
57. E. S. Cohen *et al.*, Oxidation of the alarmin IL-33 regulates ST2-dependent inflammation. *Nat. Commun.* **6**, 8327 (2015).
58. C. Bright, D. Ellis, Intracellular pH changes induced by hypoxia and anoxia in isolated sheep heart Purkinje fibres. *Exp. Physiol.* **77**, 165–175 (1992).
59. Y. Shirai *et al.*, An overview of the recent development of anticancer agents targeting the hif-1 transcription factor. *Cancers (Basel)* **13**, 1–21 (2021).
60. K. Takenaga, M. Akimoto, N. Koshikawa, H. Nagase, Cancer cell-derived interleukin-33 decoy receptor sST2 enhances orthotopic tumor growth in a murine pancreatic cancer model. *PLoS One* **15**, 1–18 (2020).
61. M.-H. Wasmer, P. Krebs, The role of IL-33-dependent inflammation in the tumor microenvironment. *Front. Immunol.* **7**, 682 (2017).
62. K. Sakata *et al.*, Establishment and characterization of high- and low-lung-metastatic cell lines derived from murine colon adenocarcinoma 26 tumor line. *Japanese J. Cancer Res.* **87**, 78–85 (1996).